ORIGINAL ARTICLE

Strategic Application of Epigenetic Regulators for Efficient Neuronal Reprogramming of Human Fibroblasts

Gary Stanley Fernandes[1,*], Rishabh Deo Singh[1,*], Debojyoti De[2], Kyeong Kyu Kim[1,3]

[1]*Department of Precision Medicine, Graduate School of Basic Medical Science (GSBMS), Institute for Antimicrobial Resistance Research and Therapeutics, Sungkyunkwan University School of Medicine, Suwon, Korea*
[2]*Department of Biotechnology, National Institute of Technology Durgapur, Durgapur, India*
[3]*Cellapeutics Bio, Seongnam, Korea*

Background and Objectives: Cellular reprogramming in regenerative medicine holds great promise for treating patients with neurological disorders. In this regard, small molecule-mediated cellular conversion has attracted special attention because of its ease of reproducibility, applicability, and fewer safety concerns. However, currently available protocols for the direct conversion of somatic cells to neurons are limited in clinical application due of their complex nature, lengthy process, and low conversion efficiency.

Methods and Results: Here, we report a new protocol involving chemical-based direct conversion of human fibroblasts (HF) to matured neuron-like cells with a short duration and high conversion efficiency using temporal and strategic dual epigenetic regulation. In this protocol, epigenetic modulation by inhibition of histone deacetylase and bromodomain enabled to overcome "recalcitrant" nature of adult fibroblasts and shorten the duration of neuronal reprogramming. We further observed that an extended epigenetic regulation is necessary to maintain the induced neuronal program to generate a homogenous population of neuron-like cells.

Conclusions: Therefore, our study provides a new protocol to produce neurons-like cells and highlights the need of proper epigenetic resetting to establish and maintain neuronal program in HF.

Keywords: Direct reprogramming, Patient-specific, Regenerative medicine, Dual epigenetic modification, Neurons

Introduction

With recent developments in cell-based therapy and cel-

lular reprogramming, regenerative medicine has emerged as a strong candidate for developing therapeutic interventions for several brain disorders ranging from neurodegenerative diseases to traumatic brain injuries. However, limited understanding of the tumorigenic potential of induced pluripotent stem cell (iPSC) technology and stem cell-based therapy prevents its adoption in clinical settings (1, 2). While neural stem cell therapy continues to be explored for its potential therapeutic application, its progress is often hindered by limited availability and uncertainty about the fate of transplanted cells (3, 4). Moreover, the transplantation of neurons or neural precursor cells originating from suitable immunotype-matched donors is extremely challenging (3).

Direct cellular reprogramming has emerged as an alternative therapeutic approach to overcome the existing limi-

tations of stem cell-based therapy (1, 5). To bypass the risk of tumorigenesis due to stem cell-based approaches, direct reprogramming using lineage-specific transcription has been attempted, which indeed possesses potential side effects owing to genetic manipulation by exogenous integration. To this end, direct reprogramming using small molecules that specifically modify signaling pathways and epigenetics is being used to generate functional somatic cells without genetic manipulation (5).

Small molecules have been successfully applied for reprogramming of different somatic cells to neurons because of their ability to specifically target signaling pathways (5). For instance, there are reports on small molecule-mediated conversion of human astrocytes and fibroblasts into functional neurons with a yield of up to 85% (6). For cell therapy, fibroblasts are excellent starting cells for neuronal reprogramming because of their easy availability and application in patient-specific cell-based therapy (1). However, the clinical application of reprogrammed neurons obtained from fibroblasts is often limited by low reprogramming efficiency and the generation of a heterogeneous cell population comprising non-converted fibroblasts (7). Although the efficiency is higher in fetal fibroblasts, adult fibroblasts are still refractory to transforming their identities under the same conditions, owing to hypermethylated heterochromatin associated with the age of the donor (8). On this note, heterogeneity seen during cellular reprogramming can be attributed to the incomplete epigenetic resetting which leaves behind epigenetic memory of the starting cell type (9, 10). Therefore, for the generation of a stable reprogrammed cell state, chromatin remodeling plays a key role in setting up of lineage-specific expression patterns and restricting the expression of lineage-inappropriate master regulators (11).

To bring about epigenetic remodeling resulting in an euchromatin state and thereby favoring somatic cells reprogramming, a combination of different epigenetic modifiers such as inhibitors against histone deacetylase (HDAC) histone methyltransferase (HMT), and bromodomain (BET) are widely used (12). Recent studies on cancer have highlighted the importance of the synergistic effects of HDAC and BET inhibitors for therapeutic applications (13, 14). The use of dual HDAC and BET inhibitors to convert astrocytes into neurons has been demonstrated (15). Therefore, we hypothesize that the strategic use of these two inhibitors may help in the rapid and efficient induction of neuronal program in human fibroblasts and its maintenance thereafter for generating matured neuron-like cells.

To validate this hypothesis, we used a cocktail of small molecules comprising of dual HDAC/BET inhibitors along with other signaling modulators, for the rapid and efficient generation for matured neuron-like cells from human fibroblasts. This study demonstrates that a temporal and strategic epigenetic regulation can enhance the reprogramming kinetics and generate a homogenous population of reprogrammed cells.

Materials and Methods

Cell and culture condition

Human foreskin fibroblasts were obtained from Millipore (Catalog no. SCC058). Cells were maintained as per the protocol in Dulbecco's Modified Eagle Medium (DMEM) (Gibco, Thermo Fisher Scientific, Inc., Waltham, MA, USA), 10% fetal bovine serum (FBS) (Gibco, Thermo Fisher Scientific, Inc., Waltham, MA, USA), and 1% penicillin-streptomycin (P/S) (Welgene, Inc., Gyeongsan, Korea).

Pre-treatment of coverslips and protein coating for cell culture

Glass coverslips were pretreated as previously described by Richner et al. (16). In brief, the coverslips were washed with detergent followed by washing with distilled water (DW) six times for 30 mins each. After washing, coverslips were dehydrated using 95% ethanol for 2 hrs before overnight treatment with nitric acid. Thereafter, the cover slips were washed 6 times with DW, 30 mins each, and were UV sterilized. Before their use for cell culture, glass coverslips were coating with 1μg/ml laminin (Sigma-Aldrich, Inc., Saint Louis, MO, USA) in $1 \times$PBS for 4 hrs.

Protocol for converting human fibroblast to neurons

Human fibroblasts were cultured on pretreated and laminin-coated 12 mm coverslips at a seeding density of 25,000 to 30,000 cells per well of a 24-well plate in DMEM, 10% FBS, and 1% P/S, one day prior to neuronal induction. For the direct conversion of HF to neuron-like cells, three different protocols were generated and tested. In the protocol 1 of neuronal conversion, the seeded cells in the first step were treated with a chemical cocktail containing small molecules 0.5 μM JQ-1(+) (MedChemExpress, Monmouth Junction, NJ, USA), 10 μM CHIR99021 (MedChemExpress, Monmouth Junction, NJ, USA), 5 μM RepSox (MedChemExpress, Monmouth Junction, NJ, USA), 12.5 μM forskolin (MedChemExpress, Monmouth Junction, NJ, USA), 10 μM Y276332 (MedChemExpress, Monmouth Junction, NJ, USA), and 0.3 μM trichostatin A (TSA) (MedChemExpress, Monmouth Junction, NJ, USA) in Neurobasal Plus media (Invitrogen, Thermo fisher, Waltham, MA, USA). Additionally, the media was supplemented with

10 ng/ml of brain-derived neurotrophic factor (BDNF) (PeproTech, Cranbury, NJ, USA), 10 ng/ml of Glial Cell Line-Derived Neurotrophic Factor (GDNF) (PeproTech, Cranbury, NJ, USA), 10 ng/ml of Neurotrophin-3 (NT3) (PeproTech, Cranbury, NJ, USA) and 0.5×B27 (Invitrogen, Thermo fisher, Waltham, MA, USA). Two days of treatment during the first step was followed by the next maturation step which contained 12.5 μM forskolin, 5 μM CHIR99021, and 10 μM Y27632, and growth factors such as 10 ng/ml basic fibroblast growth factor (bFGF) (Pepro-Tech, Cranbury, NJ, USA), 10 ng/ml BDNF, 10 ng/ml GDNF, 10 ng/ml NT3, 0.5×B27 and 1×N_2 (Invitrogen, Thermo fisher, Waltham, MA, USA) in Neurobasal Plus media for four days.

The protocol 2 for the induction of neuronal program and generation of homogenous neuron-like MAP2^+ cells involved a two-step epigenetic resetting process. The first step of neuronal induction (NI) was similar to the first step of protocol 1 with BDNF, GDNF and 0.5×B27 replaced by 2 μM retinoic acid (RA) (MedChemExpress, Monmouth Junction, NJ, USA) and 10 ng/ml bFGF. After two days, the cells were treated with extended epigenetic regulation (EER) media containing Neurobasal Plus supplemented with small molecules such as 0.3 μM JQ-1(+), 5 μM CHIR99021, and 10 μM Y27632, and growth factors which included 50 ng/ml Insulin Growth Factor 1 (IGF-1) (PeproTech, Cranbury, NJ, USA), 10 ng/ml bFGF, 20 ng/ml NT3, 100 μM N^6, 2'-O-Dibutyryladenosine 3', 5'-cyclic monophosphate (dbcAMP) (Sigma-Aldrich, Inc., Saint Louis, MO, USA), and 1×N_2 for four days.

Protocol 3 was designed to generate MAP2$^+$/NeuN$^+$/vGLUT1$^+$ neuron-like cells from MAP2$^+$/NeuN$^-$ cells generated from protocol 2. After the two-step strategic epigenetic regulation, the MAP2$^+$/NeuN$^-$ cells neuron like cells on day 6 were treated with neuronal maturation (NM) media comprising Neurobasal Plus media supplemented with small molecules such as 5 μM forskolin, 5 μM Y27632, 2 μM SP600125 (MedChemExpress, Monmouth Junction, NJ, USA), 0.5 μM dorsomorphin (MedChemExpress, Monmouth Junction, NJ, USA), 0.5 μM LDN193189 (MedChemExpress, Monmouth Junction, NJ, USA), and growth factors such as 50 ng/ml IGF-1, 20 ng/ml BDNF, NT3 10 ng/ml, GDNF 20 ng/ml, 100 μM dbcAMP, 1× L-Glutamax (Gibco, Thermo Fisher Scientific, Inc., Waltham, MA, USA), 200 mM Vitamin C (Sigma-Aldrich, Inc., Saint Louis, MO, USA), Laminin 1 μg/ml (Sigma-Aldrich, Inc., Saint Louis, MO, USA) and 1×N_2 supplement.

Conversion efficiency and neuronal purity

Conversion efficiency was calculated as previously de-

scribed (15). Briefly, we randomly selected 4~6 view fields for each sample on day two post neuronal induction using an Olympus IX-51 microscope and counted the total number of TUJ1$^+$/DAPI and DCX$^+$/DAPI. The conversion efficiency was calculated as the ratio of TUJ1$^+$/DAPI cells and DCX$^+$/DAPI to the initial number of seeded cells in each visual field. The neuronal purity represents the percentage of MAP2$^+$ cells on day six in total cells stained by DAPI (15). Quantitative data are presented as the mean± SEM of at least three independent experiments.

RNA isolation and cDNA synthesis

Cells were harvested from three wells of 24-well plates at the indicated time points, and total RNA was extracted using RNeasy Mini Kit (QIAGEN, Hilden, Germany), for a total of 50~100 ng/μl of pure RNA. The isolated RNA had an A260/A280 ratio between 1.8 to 2.1, which indicates RNA purity. The isolated RNA was stored at -8 0°C. For cDNA synthesis, a One-Script$^{\circledR}$ cDNA Synthesis Kit (abm, Vancouver, Cananda) was used to convert 2 μg of RNA to cDNA in a total reaction volume of 20 μl.

RT-qPCR analysis

RT-qPCR was performed using SYBR Green PCR Master Mix (Bio-Rad, Bio-Rad Laboratories, Inc., Hercules, CA, USA) on a Bio-Rad Prime PCR instrument. The qRT-PCR conditions were 40 cycles of 30 s at 95°C, 15 s at 60°C, and 15 s at 72°C. The primers used in these studies are listed in Supplementary Table S1.

Immunostaining

For cell staining, cultures were washed twice with 1× phosphate-buffered saline (PBS) (Welgene, Republic of Korea) and fixed in 4% formaldehyde (Sigma-Aldrich, Inc., Saint Louis, MO, USA) in PBS for 15 min at room temperature. The cells were then washed thrice with 1× PBS and permeabilized with 0.1% Triton-X-100 (USB Corporation, OH, USA) in PBS for 10 min at room temperature. The cells were washed thrice with 1×PBS and blocked with a blocking solution containing 1% bovine serum albumin (BSA) (Amresco, France), 22.52 mg/ml glycine (Affymetrix, CA, USA), and 0.1% Tween 20 (Affymetrix, CA, USA) in PBS for 60 mins. Subsequently, the cells were incubated with primary antibodies diluted in dilution solution containing 1% BSA (Amresco, France) and 0.1% Tween 20 (Affymetrix, CA, USA) overnight at 4°C. The cells were then washed thrice with 1× PBS containing 0.1% Tween-20 (PBST) and incubated with secondary antibodies for 2 h at room temperature. Cells were then washed thrice with PBST and incubated with 1 μg/ml

DAPI (Sigma-Aldrich, MO, USA) for 5 min at room temperature to stain the nuclei. The samples were subsequently visualized using a fluorescence microscope (IX71S1F3, Olympus, Japan). All antibodies used in this study are listed in Supplementary Table S2.

Calcium staining

Calcium imaging was performed on $MAP2^+/NeuN^+/vGLUT1^+$ neuron-like cells derived from human fibroblast using Rhoda-2-AM (Sigma-Aldrich, Inc., Saint Louis, MO, USA) at a concentration of 2 μM. Imaging was performed in Live-Imaging Solution (Invitrogen, Thermo Fisher Scientific, Inc., Waltham, MA, USA). Images were acquired at 30 frames/s using a scientific CMOS camera. The microscope was controlled by Micro-Manager software and the image processor ImageJ. The samples were visualized using fluorescence microscopy (IX71S1F3, Olympus, Tokyo, Japan). Changes in fluorescence were measured for individual cells, and the average of the first 10 time-lapse images for each region of interest (ROI) was defined as the initial fluorescence (F_0).

Results

Chemical cocktail containing dual HDAC/BET inhibitors induces neuronal programming in human fibroblasts

Current protocols for generating neurons from fibroblasts exploit the reprogramming potential of epigenetic modifiers using inhibitors against HDAC or BET alone (7, 17-21). The use of dual HDAC/BET inhibitors instead of using one inhibitor for reprogramming human somatic cells into neurons has been demonstrated to induce epigenetic plasticity in human adult astrocytes, which resulted in improved neuronal conversion (15). Therefore, we hypothesized that human fibroblasts that resist neuronal reprogramming like human adult astrocytes do, could show improved neuronal efficiency upon application of dual HDAC/BET inhibitors.

For our study, we used human fibroblast (HF) cells, the identity of which was confirmed by in-house characterization. The staining results indicated that the HF cells did not contain any neuronal contaminants (Supplementary Fig. S1A and S1B). To prove our hypothesis regarding the rapid and efficient generation of neurons by applying the dual epigenetic regulation strategy, we developed a small-molecule chemical cocktail with dual HDAC/BET inhibitors, comprising HDAC inhibitor trichostatin A (TSA), and BET inhibitor JQ-1(+). In addition, we supplemented these epigenetic modifiers with other small molecules re-

ported to promote neuronal reprogramming (7, 18), such as forskolin (cAMP activator), CHIR99021 (WNT activator), Y27632 (ROCK inhibitor), and RepSox (TGF-b inhibitor), constituting a cocktail referred to as 6C (Fig. 1A). HF cells treated with 6C cocktail along with growth factors BDNF, GDNF, NT3, and 0.5×B27 (Neuronal induction of protocol 1, Fig. 1A) generated a morphological change over a period of two days, showing a shrinkage of the soma and loss of fibroblast-like morphology (Day 2, Fig. 1B).

The ability of these six small molecules to induce neuronal reprogramming was confirmed by the presence of the early neuronal markers TUJ1 and DCX on day two with an efficiency of 88±4% and 71±3% respectively (Fig. 1C and 1D). Furthermore, real-time quantitative PCR (RT-qPCR) analysis showed upregulation of genes related to neuronal reprogramming and downregulation of fibroblast-associated markers (Fig. 1E and Supplementary Fig. S1C).Taken together, our data demonstrate that the usage of two epigenetic modifiers together in combination with small molecules to modulate signaling pathways could rapidly and efficiently induce neuronal programming.

Role of individual epigenetic modifiers in neuronal induction

The use of 6C with dual HDAC/BET inhibitors instigated rapid and efficient induction of $TUJ1^+/DCX^+$ cells after two days of treatment. To highlight the importance of this temporal dual epigenetic regulation used in the first step, we compared the arrival of DCX expression after two days of treatment with the complete cocktail to the cocktail with only one or none of the epigenetic modifiers. Only bFGF was supplemented to the media to ensure the cell survived under the exposure of aforementioned small molecules (22). The removal of any of the epigenetic regulators significantly affected the neuronal induction efficiency of the cocktail as evident by the number of DCX^+ cells and the change in the morphology of cells generated after two days (Fig. 2A and 2B). TSA was found to be the key regulator as its removal resulted to a significant drop in neuronal reprogramming efficiency with only 8±4% cells showing DCX expression. The removal of JQ-1(+) from the 6C cocktail resulted to a reprogramming efficiency of 34±9% which is nearly half of DCX^+ cells generated by 6C cocktail, 67±2% (Fig. 2C), when treated only in the presence of bFGF. Furthermore, the neuronal reprogramming efficiency in the absence of both the epigenetic modifiers was found to be 11±5% and the number of DCX^+ cells in the media control was negligible. Taken together, our results highlight the importance of each of the epigenetic modifiers in the cocktail
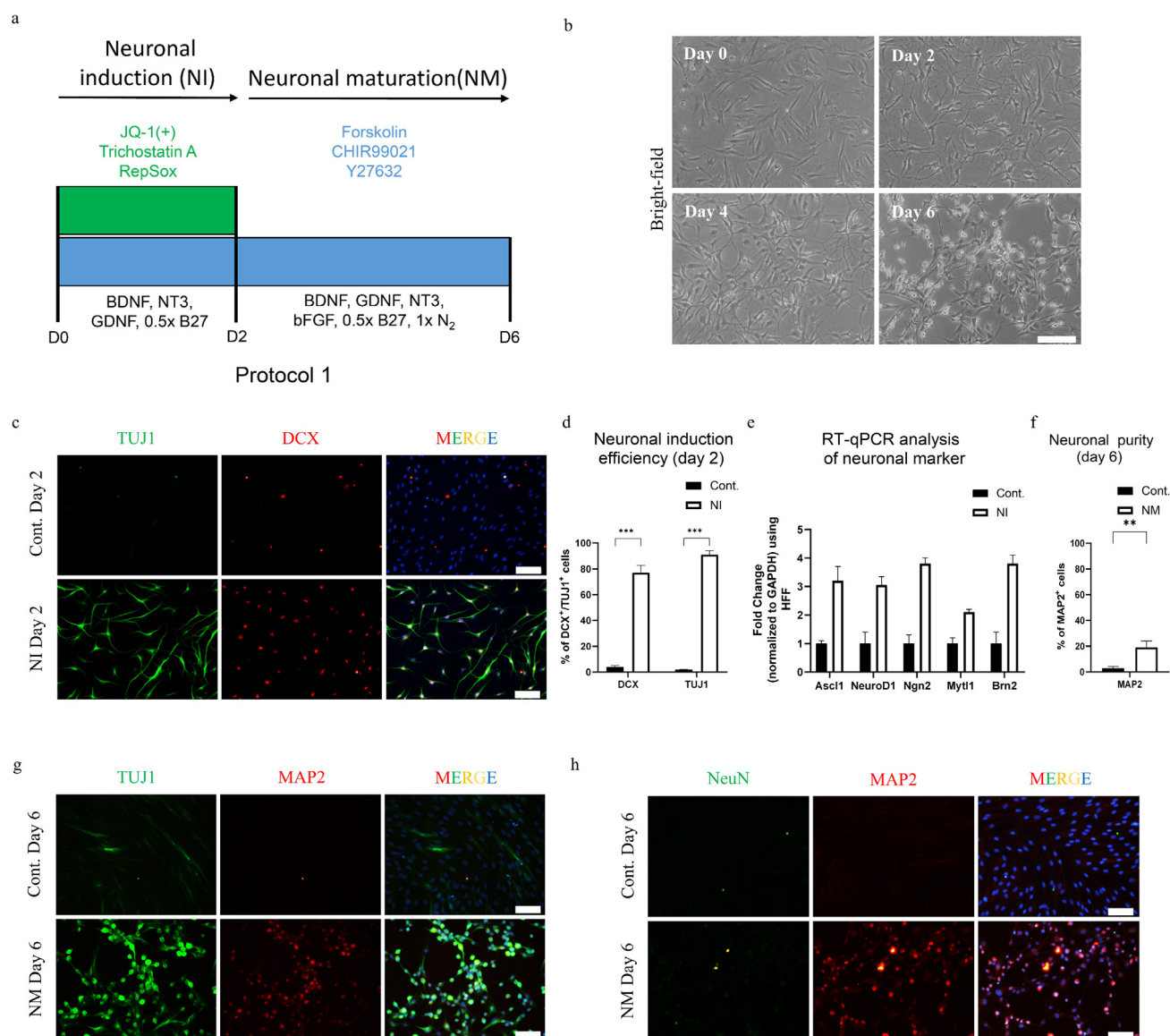
Fig. 1. Dual HDAC/BET inhibitors for the induction of neuronal programming. (a) Schematic design of protocol 1 for the neuronal conversion of human fibroblast into neurons. (b) Bright-field images showing the morphological changes of cells over six days using neuronal induction and neuronal maturation protocol. Scale bar, 100 μm. (c) TUJ1 and DCX immunostaining of human fibroblast cells after two days of exposure to 6C. Scale bar, 100 μm. (d) Neuronal induction efficiency two days after the treatment with 6C cocktail normalized to control human fibroblast culture on day zero. (e) mRNA levels of key genes related to neuronal reprogramming as assessed by RT-qPCR on day two. (f) Neuronal purity on day six as percentage of MAP2$^+$ cells. (g) TUJ1 and MAP2 immunostaining on day six after treatment with 6C and FCY. Scale bar, 100 μm. (h) NeuN and MAP2 immunostaining on day six after treatment with 6C and FCY. Scale bar, 100 μm. The merge image shows the overlap of neuronal markers with the nucleus stained by DAPI. Statistical differences were examined by student's t-test, **p<0.001, and ***p<0.0001.

and demonstrated a preliminary level of evidence of the synergistic effect of dual HDAC/BET inhibition for the rapid and efficient induction of neuronal program.

Removal of epigenetic regulator after two days of induction generates small pool of early neuron-like cells

Upon TUJ1 and DCX expression after two days of 6C treatment, we introduced another step of neuronal maturation for the maintenance and maturation of induced early neurons (Fig. 1A). In an attempt to generate matured neu-
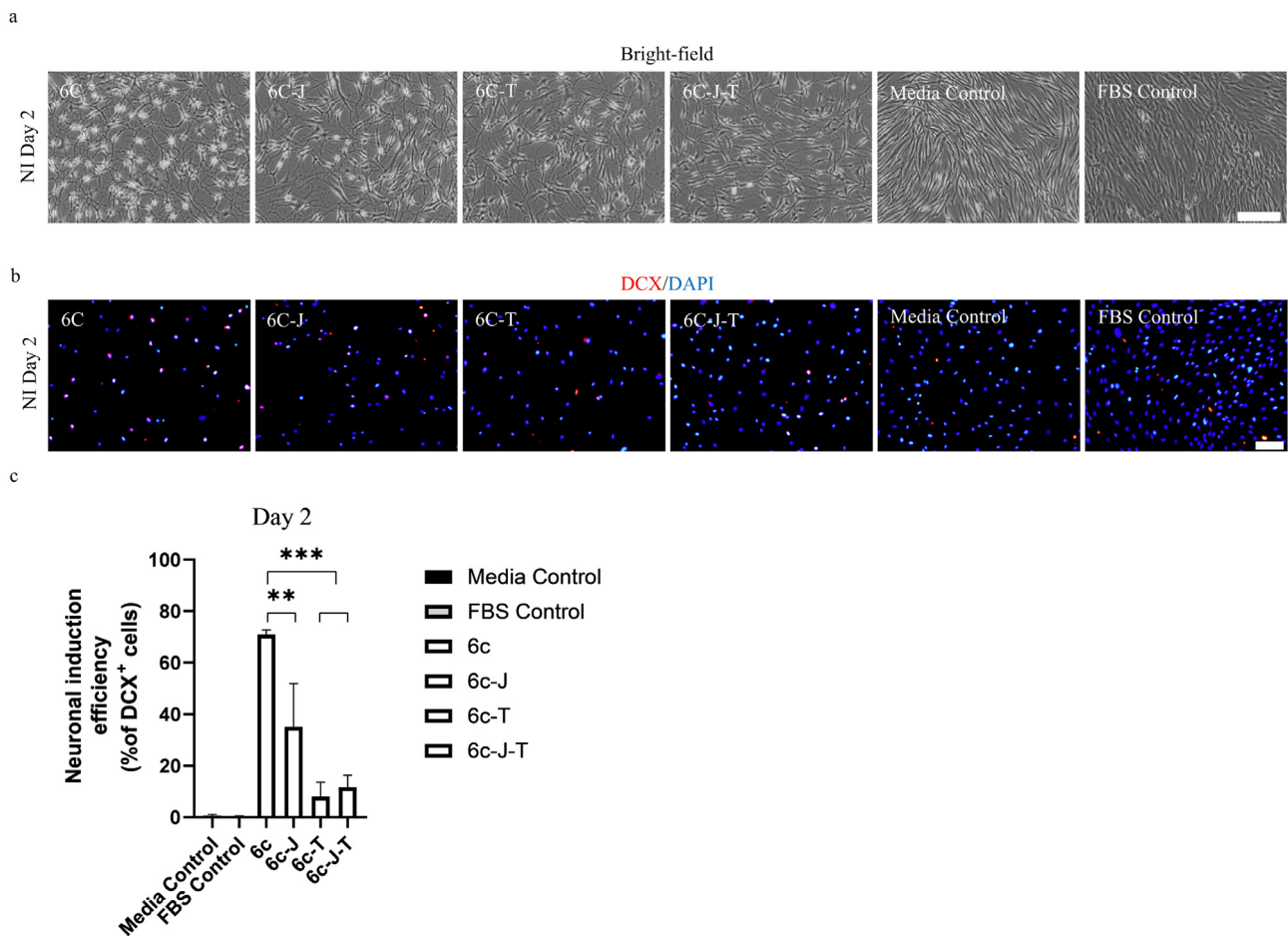
Fig. 2. Role of individual epigenetic modifiers in neuronal induction. (a) Representative bright-field image of induced human fibroblast cells to investigate the role of epigenetic regulators by individually removing them from 6C. Scale bar, 100 μm. (b) DCX immunostaining of the human fibroblast cells treated with complete 6C cocktails and when epigenetic modifiers are removed from 6C cocktail, Scale bar, 100 μm. The figure shows the overlap of DCX and DAPI. (c) Neuronal induction efficiency determined on day two post neuronal induction normalized to control human foreskin culture day. Statistical differences were examined by one way ANOVA with Dennett's post hoc test, **p<0.002, and ***p<0.001.

rons from $TUJ1^+/DCX^+$ induced early neurons, we adopted a reduction approach by removing the chemicals from the 6C cocktail. In addition to removing the epigenetic modifiers because of their ability to induce toxicity, we removed RepSox because of its known role in promoting Sox2 expression during the formation of a pluripotent stage (23). The resultant maturation cocktail comprising forskolin, CHIR99021, and Y27632 (FCY) promoted cell survival, with few cells showing typical neuron-like morphology (D6, Fig. 1B) with an abundance of non-reprogrammed, fibroblast-like cells. The neuronal purity after six days, defined by the percentage of $MAP2^+$, was found to be approximately 19±5% along with the expression of pan-neuronal marker TUJ1 (Fig. 1F and 1G). However, the expression of another mature marker, NeuN, was negligible after

six-day treatment (Fig. 1H). A detailed morphological analysis of the cells at day 6 revealed that most $MAP2^+$ cells lacked proper neurite extension (Fig. 1G). Moreover, an extended incubation with FCY beyond day 6 did not improve the neuronal morphology (Supplementary Fig. S1D). These results suggested the requirement for a modification in the chemical cocktail to generate a homogenous population of mature neuron-like cells.

Extended BET inhibition is required for the maintenance of neuronal program

Since the FCY treatment in the second step of protocol 1 generated neurons with very low purity, we investigated numerous other chemical combinations for their ability to maintain neuronal maturation and purity beyond the in-

duction state (Supplementary Fig. S2). Interestingly, one condition containing JQ-1(+) was found to be effective in promoting neurite extension and maintaining the purity. These results suggested the requirement of an extended epigenetic remodeling (ERR) for the sustenance of the neuronal program and preventing the generation of non-reprogrammed cells. Hypothetically, the epigenetic regulation in the first induction step of two days in the protocol 1 was sufficient to trigger gene expression responsible for neuronal induction, but those involved in the neuronal maturation were not optimally expressed and the epigenetic resetting favoring neuronal-lineage was not stable. We found that a cocktail containing JQ-1(+), CHIR99021 and Y27632 (JCY) resulted in the generation of neuron-like cells having proper soma with well-defined elongated neurites which is a typical neuronal morphology (24). In addition, the presence of non-reprogrammed fibroblast-like cells was minimal as compared to the other condition showing excellent morphological homogeneity (Supplementary Fig. S2); however, with a certain level of toxicity. We reduced this JCY-induced toxicity using appropriate growth factors which included dbCAMP, IGF-1, NT3, bFGF and N_2 during the two-step epigenetic regulation (Fig. 3A and 3B). Moreover, we further improved the induction proto-
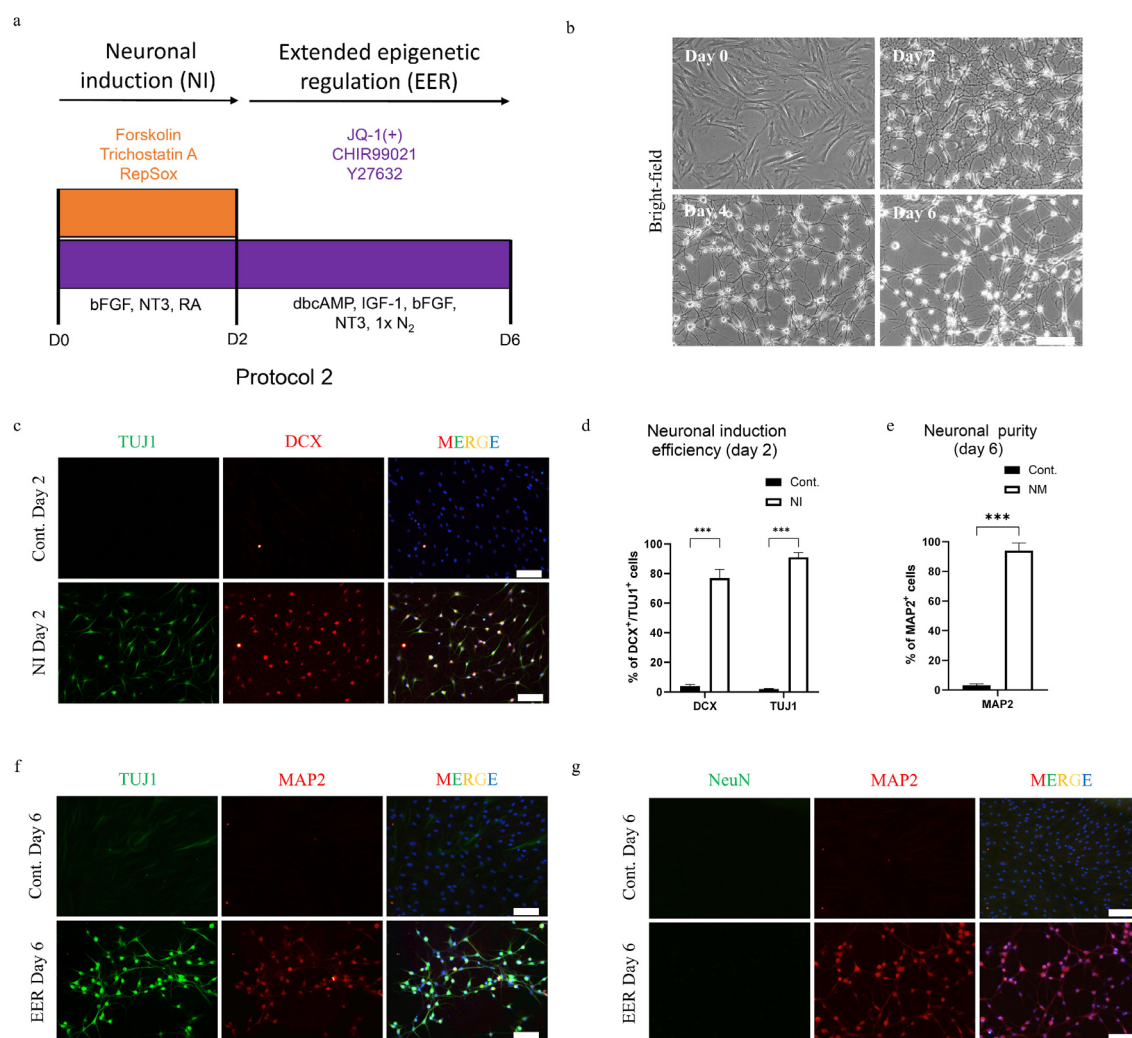

Fig. 3. Extended BET inhibition for generating a homogenous population. (a) Schematic design of two-step protocol 2 for converting human fibroblast into neurons. (b) Bright-field images showing the morphological changes over six days of neuronal reprogramming. (c) TUJ1 and DCX immunostaining after two days of exposure to 6C. Scale bar, 100 μm. (d) Neuronal induction efficiency two days after the treatment with 6C cocktail normalized to control human culture on day zero. (e) Neuronal purity on day six as percentage of MAP2$^+$ cells. (f) TUJ1 and MAP2 immunostaining on day six after treatment with 6C and JYC. Scale bar, 100 μm. (g) MAP2 and NeuN immunostaining on day six after treatment with 6C and JYC. Scale bar, 100 μm. The merge image shows the overlap of neuronal markers with the nucleus stained by DAPI. Statistical differences were examined by student's t-test, ***$p < 0.0001$.

col by replacing GDNF, BDNF and B27 used during the first two days with Retinoic acid (RA) and bFGF. The introduction of RA and bFGF during the first two days resulted in the brightening of the cell soma which resembles to the reported neuronal morphology (7); however the in-

duction efficiency remained similar (TUJ1$^+$ cells 91±2% and DCX$^+$ 75±7%) in comparison to Protocol 1 (TUJ1$^+$ cells 88±4% and DCX$^+$ cells 71±3%) (Fig. 3B, 3D and 1D). Finally, we standardized a new two-step protocol comprising of neuronal induction for two days followed by
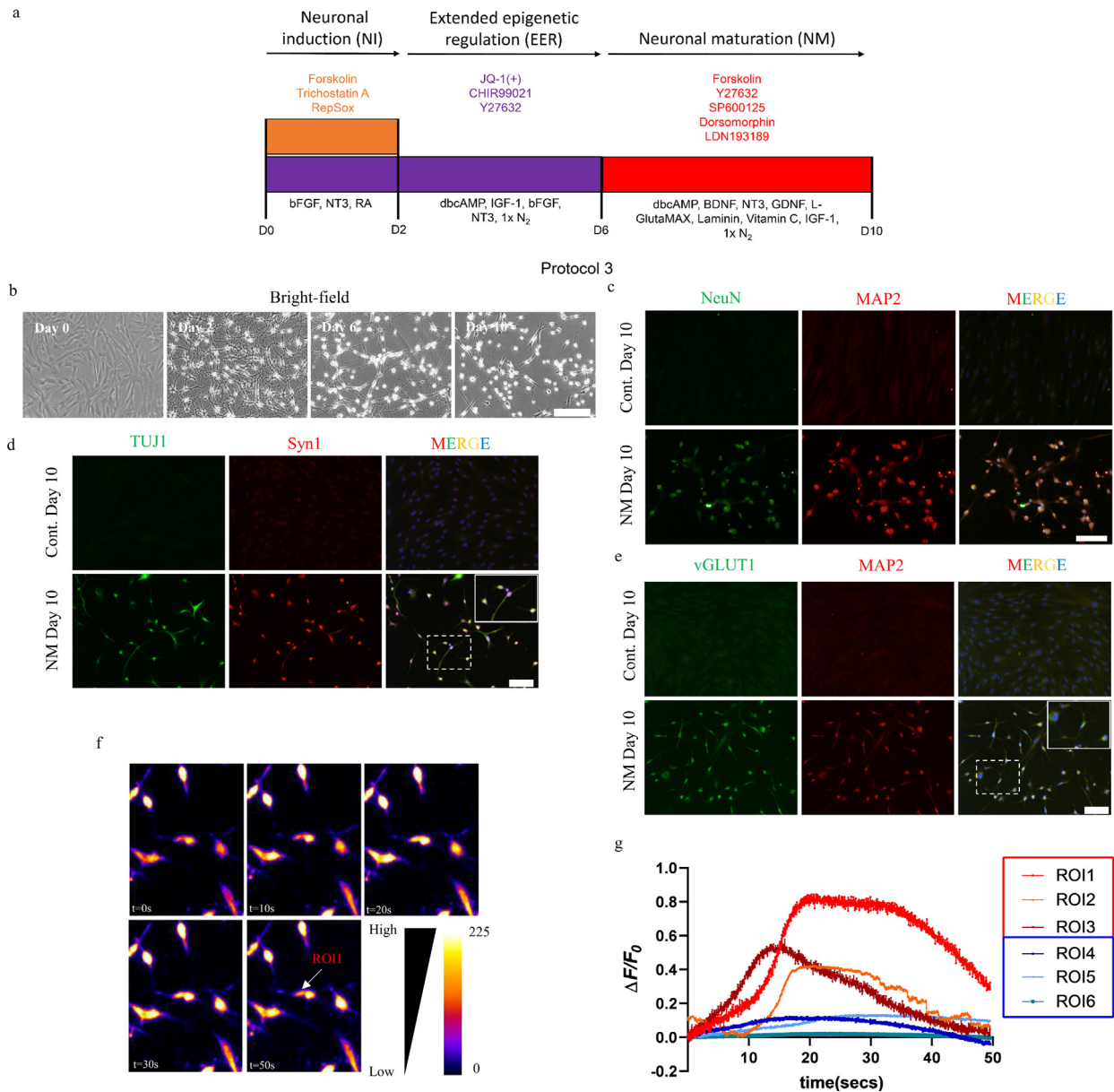

Fig. 4. Maturation cocktail for the generation of mature neuron-like cells. (a) Schematic design of protocol 3 for the generation of mature and functional neurons. (b) Bright-field images showing the morphological changes over 10 days of the generation of MAP2$^+$/NeuN$^+$/vGlUT1$^+$ neuron-like cells. Dual immunostaining of neuron-like cells at day 10 with following markers; (c) NeuN and MAP2, (d) TUJ1 and Syn1, and (e) vGLUT1 and MAP2. Scale bar, 100 μM. The merge image shows the overlap of neuronal markers with the nucleus stained by DAPI. The boxes in lower most right panels show the magnified image of the indicated regions. (f) Fluorescent images of cells loaded with Rhod 2-AM after different time intervals for 50 sec. The arrow indicates the representative region (ROI 1) in which fluorescence intensity was measured. (g) A plot of $\Delta F/F_0$ showing the change in fluorescent intensity over time with respect to the initial fluorescence for different ROIs as the one demonstrated in panel f. ROI 1~6 were picked on the basis of change in the fluorescence intensity over time and the neuronal morphology as stained by the dye. Selected pseudo-color frames are baseline subtracted images (ΔF) of the cell.

the maintenance of neuronal program using an extended epigenetic regulation approach (Protocol 2, Fig. 3A).

The neuron-like cells generated by our new two-step protocol (Protocol 2) showed obvious morphological differences from those induced by protocol 1 (Fig. 3B Day 6 vs. Fig. 1B Day 6). By applying the new protocol, we were able to generate a large pool of cells with a high neuronal purity of 91±3% (MAP2$^+$ cells) (Fig. 3E) co-expressing TUJ1 and MAP2 (Fig. 3F). However, the expression of the matured marker NeuN was still lacking (Fig. 3G). Taken together, our results demonstrated the need of an extended BET inhibition for the maintenance of the neuronal program and generation of a homogenous neutron-like population for their further maturation.

Neuronal maturation cocktail to generate mature NeuN$^+$/vGLUT1$^+$/Syn1$^+$ neurons

The continued exposure of the cocktail JYC beyond six days did not promote NeuN expression but resulted in cell toxicity and loss of neuronal morphology (Supplementary Fig. S3A and S3B). Moreover, the application of neuronal maturation cocktail from protocol 1 resulted to similar outcome as seen with JYC (Supplementary Fig. S3A and S3C). One of the possible explanations for the neurons not showing NeuN expression upon extended JYC treatment is the role of JQ-1(+) in suppressing nuclear factor kappa B (NF-κB) which is important for neuronal development and synaptic activation (25, 26). To circumvent this issue and generate fully matured neurons, we included an additional neuronal maturation step after EER with a chemical cocktail comprising forskolin, Y27632, LDN193189, dorsomorphin and SP600125 (FYLDSp), based on the small molecules used in previously reported protocols (7, 19), along with dbcAMP, BDNF, NT3, GDNF, IGF-1, 1× L-GlutaMAX, Vitamin C, Laminin and 1×N2 supplement (27) (Protocol 3, Fig. 4A). The addition of the new maturation step enabled cell survival for more than 10 days, allowing them to acquire proper neuronal morphology (Fig. 4B and Supplementary Fig. S3A and S3D).

Moreover, the maturation cocktail from day six promoted NeuN expression which was observed by immunostaining on day 10 (Fig. 4C). Furthermore, along with the presence of punctuated synaptic vesicles evident by Syn1 staining of neurites (Fig. 4D), we also found that nearly 64% of the cells surviving on day 10 were vGLUT1-positive (Fig. 4E).

Our maturation step using the cocktail FYLDSp generated TUJ1$^+$/MAP2$^+$/NeuN$^+$/vGLUT1$^+$ neuron-like cells, indicating that the challenges posed by JQ-1(+) during neuronal maturation can be addressed. To this end, we investigated whether these reprogrammed cells attained neu-

ronal functionality by analyzing the calcium influx/outflow, which is one of the functional properties of neurons (28, 29). Incubating the cells with Rhod 2-AM, a high affinity Ca^{2+} indicator, showed spontaneous calcium influx followed by a gradual outflow of calcium over period of 50 sec. A detailed analysis of neuron-like cells' signal pattern revealed that intracellular calcium influx and outflow are heterogeneous. We observed that 7.8% of the neuron-like cells showed sudden rise of calcium influx followed by gradual outflow after 20 seconds, which were comparable to previously described neurons showing action potential (Fig. 4F and ROI 1, ROI 2 and ROI 3 respectively in Fig. 4G) (28). However, a large number of the neuron-like cells maintained a passive influx and outflow of calcium signaling, indicating the developmental phase of the reprogrammed cells which are yet to attain full functionality (30) (ROI 4, ROI 5 and ROI 6 respectively in Fig. 4G).

To sum up, the immunostaining results showing the presence of mature neuronal markers along with the spontaneous influx and outflow of calcium demonstrate the efficacy of the maturation cocktail to generate mature neuron-like cells.

Discussion

One of the major challenges in clinical application of patient-derived cells in regenerative medicine is their efficient and time-dependent availability. To address this issue, we developed a new neuronal conversion protocol involving the application of dual HDAC/BET inhibition followed by extended BET inhibition. To our knowledge, this is the first study to show that dual epigenetic inhibition using JQ-1(+) and TSA results in a rapid induction of the neuronal program in somatic human fibroblast cells within two days. We demonstrated that our strategic epigenetic regulation effectively generated 91±2% TUJ1$^+$ and 75±7% DCX$^+$ cells within two days of treatment which otherwise takes minimum six to seven days as reported by other published protocols (Supplementary Table S3).

BET proteins, one of the best-characterized epigenetic readers, are members of the bromodomain-binding protein (BRD) family that controls gene regulation by recognizing the acetylation state of lysine residues (31). HDACs are critical epigenetic erasers, which remove acetyl groups from lysine residues in histone (32). Previous studies have highlighted synergistic and beneficial effects of this dual epigenetic regulation as a potential therapeutic approach for cancer treatment (13, 33). In addition, both epigenetic modulators used in the present study play a role in neurological disorders (32), which shows the possibility of using

them together for neuronal reprogramming. To this end, Gao et al. (15) successfully demonstrated the generation of neurons from adult human astrocytes using a chemical cocktail containing dual HDAC/BET inhibitors with an efficiency of 35% within 18 days of treatment. Accordingly, in this study, we have proved that the temporal and strategic epigenetic regulation using these inhibitors, along with other signaling molecules, can generate a homogenous population of neuron-like cells. The rapid and efficient generation of $DCX^+/TUJ1^+$ cells from human fibroblasts demonstrated the effectiveness of strategic HDAC/BET inhibition in generating cells for applicability in patient-specific regenerative medicines.

Our initial study on conversion of human fibroblasts to neurons supports the need of a proper epigenetic modifications allowing the expression of lineage-specific genes and establishing a new cell fate. Indeed, immediate withdrawal of HDAC/BET after the appearance of DCX and TUJ1 did not promote spontaneous neuronal reprogramming and resulted to non-reprogrammed fibroblast-like cells. We successfully addressed this problem including the epigenetic modifier, JQ-1(+), in an extended epigenetic regulation step (Protocol 2). As it is, we standardized a dual epigenetic regulation process using JQ-1(+) and TSA in the first induction step followed by an extended epigenetic regulation step using JQ-1(+), in combination with other signaling molecules. Indeed, using this new protocol, we generated a large pool of neuron-like cells with $TUJ1^+$ /$MAP2^+$ although these cells showed negligible expression of NeuN, a known marker of mature neurons.

Generating mature $MAP2^+/NeuN^+$ neuron-like cells was challenging because of the effects exerted by JQ-1(+). JQ-1(+), through BRD4 downregulation, downregulates immediate early genes that are associated with synapse formation and neuronal signal transmission (34). Additionally, the NF-κB pathway, associated with synaptic plasticity and formation, has also been reported to be adversely affected by BRD4 inhibition using JQ-1(+) (25, 35). Indeed, withdrawal or long-term use of JQ-1(+) resulted in a significant loss of neuronal morphology accompanied by a gain in fibroblast-like morphology. An additional maturation cocktail containing the molecules FYLDSp resulted in the neuronal maturation process, as evident by NeuN expression and calcium signaling. The presence of somatic calcium signaling in such cells demonstrates their action potential, which has been defined as an integral part of the functionality of mature synapses present within the neural circuit (36). The calcium signaling pattern and $\varDelta F/(F_0)$ observed in $MAP2^+/NeuN^+$ neuron-like cells were in line with previously reported studies involving early developing

iPSCs-based neurons and primary neurons from Drosophila (30, 37). From a neuronal development point of view, intracellular calcium signaling in the form of transient calcium spikes and waves are known to regulate neuronal growth, survivability and synapse formation (38, 39).

Although we have highlighted the need for a strategic epigenetic regulation for the rapid induction and further maintenance of neuronal program, our study herein has potential limitations. Our calcium staining analysis revealed that 7.8% of induced neuron-like cells showed somatic intracellular staining reflecting their potential to form synapse connections and build neural circuitry although (30) most converted cells expressed the key neuronal markers. However, in previously reported protocols, a higher percentage of reprogrammed neurons have been shown to exhibit electrophysiological properties when analyzed at various time points (Supplementary Table S3). Moreover, the culture of reprogrammed cells in the maturation cocktail beyond day 10 resulted to a gradual cell lost. Hence, to promote survival and ensure that a larger population of neuron-like cells acquire maturity and thus attain functionality for therapeutic application, the culture condition of the obtained neuron-like cells needs to be further optimized to ensure long-term survivals. In spite of the presence of key maturation markers, studies have highlighted the need for prolonged culturing of reprogrammed neuronal cells to acquire complete functionality in terms of transient calcium spikes, synapse formation and the building of neural-circuit (30). Hence, we hypothesize that a culture condition which can maintain $TUJ1^+/MAP2^+/NeuN^+/vGLUT1^+$ neuron-like cells for longer time period may result in the higher percentage of cells showing somatic calcium signaling and synapse formation. In addition to this, an epigenome analysis is required to validate the role of HDAC/BET inhibition in the remodeling of chromatin encompassing neural lineage genes for the rapid induction of neuronal program. Furthermore, the role of BET inhibition in guiding the reprogramming trajectory to generate a homogenous population and maturation of neuron-like cells has to be elucidated. It will be interesting to know how JQ-1(+) remodels the epigenetics to promote the expression of neuronal maturation related genes.

From a therapeutic point of view, cellular transplantation of early neurons prior to being committed towards a neuronal specification/subtype are considered to have a much higher potential of tissue integration (40). In this regard, we hypothesize that the $MAP2^+/Tuj1^+$ neuron-like cells obtained at day 6 could find potential use in cell transplantation therapy. Such time points have also been

used in previously published reports. For instance, Gao et al. have successfully demonstrated *in vivo* cell transplantation of small molecule induced neurons from human astrocytes post 6 days neuronal induction despite the protocols neuronal induction process being described as complete after 18 days (15).

In conclusion, we here report the use of HDAC and BET epigenetic modulation for the efficient and rapid reprogramming of human fibroblasts into neuron-like cells. The application of chemical cocktail containing dual HDAC/BET inhibition for the neuronal induction, followed by an extended BET inhibition for maintaining the neuronal program generated a homogenous population of $MAP2^+$ cells with a purity of $91\pm3\%$. The treatment of these cells with maturation cocktail generated $NeuN^+/vGLUT1^+/Syn1^+$ mature neuron-like cells. This temporal need of epigenetic regulation highlights the need for appropriate epigenetic resetting for the induction and sustenance of lineage-specific program. Thus, our strategic epigenetic regulation can be a plausible approach for the efficient generation of neuron-like cells which can be used to develop new therapeutic intervention for the treatment of neurodegenerative diseases.

Acknowledgments

Potential Conflict of Interest

Some of current results are patent pending.

Supplementary Materials

Supplementary data including three tables and three figures can be found with this article online at https://doi.org/10.15283/ijsc22183.

References

1. Kim Y, Jeong J, Choi D. Small-molecule-mediated reprogramming: a silver lining for regenerative medicine. Exp Mol Med 2020;52:213-226
2. De D, Halder D, Shin I, Kim KK. Small molecule-induced cellular conversion. Chem Soc Rev 2017;46:6241-6254
3. Aron Badin R, Bugi A, Williams S, Vadori M, Michael M, Jan C, Nassi A, Lecourtois S, Blancher A, Cozzi E, Hantraye P, Perrier AL. MHC matching fails to prevent long-term rejection of iPSC-derived neurons in non-human primates. Nat Commun 2019;10:4357
4. Medvedev SP, Shevchenko AI, Zakian SM. Induced pluripotent stem cells: problems and advantages when applying them in regenerative medicine. Acta Naturae 2010;2:18-28
5. Xie X, Fu Y, Liu J. Chemical reprogramming and transdifferentiation. Curr Opin Genet Dev 2017;46:104-113
6. Zhang L, Yin JC, Yeh H, Ma NX, Lee G, Chen XA, Wang Y, Lin L, Chen L, Jin P, Wu GY, Chen G. Small molecules efficiently reprogram human astroglial cells into functional neurons. Cell Stem Cell 2015;17:735-747
7. Yang Y, Chen R, Wu X, Zhao Y, Fan Y, Xiao Z, Han J, Sun L, Wang X, Dai J. Rapid and efficient conversion of human fibroblasts into functional neurons by small molecules. Stem Cell Reports 2019;13:862-876
8. Sturm G, Cardenas A, Bind MA, Horvath S, Wang S, Wang Y, Hägg S, Hirano M, Picard M. Human aging DNA methylation signatures are conserved but accelerated in cultured fibroblasts. Epigenetics 2019;14:961-976
9. Zwaka TP. Stem cells: troublesome memories. Nature 2010;467:280-281
10. Biddy BA, Kong W, Kamimoto K, Guo C, Waye SE, Sun T, Morris SA. Single-cell mapping of lineage and identity in direct reprogramming. Nature 2018;564:219-224
11. Papp B, Plath K. Epigenetics of reprogramming to induced pluripotency. Cell 2013;152:1324-1343
12. Jaenisch R, Bird A. Epigenetic regulation of gene expression: how the genome integrates intrinsic and environmental signals. Nat Genet 2003;33 Suppl:245-254
13. He S, Dong G, Li Y, Wu S, Wang W, Sheng C. Potent dual BET/HDAC inhibitors for efficient treatment of pancreatic cancer. Angew Chem Int Ed Engl 2020;59:3028-3032
14. Ren Q, Gao W. Current status in the discovery of dual BET/HDAC inhibitors. Bioorg Med Chem Lett 2021;38:127829
15. Gao L, Guan W, Wang M, Wang H, Yu J, Liu Q, Qiu B, Yu Y, Ping Y, Bian X, Shen L, Pei G. Direct generation of human neuronal cells from adult astrocytes by small molecules. Stem Cell Reports 2017;8:538-547
16. Richner M, Victor MB, Liu Y, Abernathy D, Yoo AS. MicroRNA-based conversion of human fibroblasts into striatal medium spiny neurons. Nat Protoc 2015;10:1543-1555
17. Yang J, Cao H, Guo S, Zhu H, Tao H, Zhang L, Chen Z, Sun T, Chi S, Hu Q. Small molecular compounds efficiently convert human fibroblasts directly into neurons. Mol Med Rep 2020;22:4763-4771
18. Hu W, Qiu B, Guan W, Wang Q, Wang M, Li W, Gao L, Shen L, Huang Y, Xie G, Zhao H, Jin Y, Tang B, Yu Y, Zhao J, Pei G. Direct conversion of normal and Alzheimer's disease human fibroblasts into neuronal cells by small molecules. Cell Stem Cell 2015;17:204-212
19. Li X, Zuo X, Jing J, Ma Y, Wang J, Liu D, Zhu J, Du X, Xiong L, Du Y, Xu J, Xiao X, Wang J, Chai Z, Zhao Y, Deng H. Small-molecule-driven direct reprogramming of mouse fibroblasts into functional neurons. Cell Stem Cell 2015;17:195-203
20. Qin H, Zhao AD, Sun ML, Ma K, Fu XB. Direct conversion of human fibroblasts into dopaminergic neuron-like cells using small molecules and protein factors. Mil Med

Res 2020;7:52

21. Wan XY, Xu LY, Li B, Sun QH, Ji QL, Huang DD, Zhao L, Xiao YT. Chemical conversion of human lung fibroblasts into neuronal cells. Int J Mol Med 2018;41:1463-1468

22. Shaulian E, Resnitzky D, Shifman O, Blandino G, Amsterdam A, Yayon A, Oren M. Induction of Mdm2 and enhancement of cell survival by bFGF. Oncogene 1997;15:2717-2725

23. Ichida JK, Blanchard J, Lam K, Son EY, Chung JE, Egli D, Loh KM, Carter AC, Di Giorgio FP, Koszka K, Huangfu D, Akutsu H, Liu DR, Rubin LL, Eggan K. A small-molecule inhibitor of tgf-Beta signaling replaces sox2 in reprogramming by inducing nanog. Cell Stem Cell 2009;5:491-503

24. He S, Guo Y, Zhang Y, Li Y, Feng C, Li X, Lin L, Guo L, Wang H, Liu C, Zheng Y, Luo C, Liu Q, Wang F, Sun H, Liang L, Li L, Su H, Chen J, Pei D, Zheng H. Reprogramming somatic cells to cells with neuronal characteristics by defined medium both in vitro and in vivo. Cell Regen 2015;4:12

25. Boersma MC, Dresselhaus EC, De Biase LM, Mihalas AB, Bergles DE, Meffert MK. A requirement for nuclear factor-kappaB in developmental and plasticity-associated synaptogenesis. J Neurosci 2011;31:5414-5425

26. Hajmirza A, Emadali A, Gauthier A, Casasnovas O, Gressin R, Callanan MB. BET family protein BRD4: an emerging actor in NFκB signaling in inflammation and cancer. Biomedicines 2018;6:16

27. Masserdotti G, Gascón S, Götz M. Direct neuronal reprogramming: learning from and for development. Development 2016;143:2494-2510

28. Irwin RP, Allen CN. Simultaneous electrophysiological recording and calcium imaging of suprachiasmatic nucleus neurons. J Vis Exp 2013;(82):50794

29. Fernandes GS, Singh RD, Kim KK. Generation of a pure culture of neuron-like cells with a glutamatergic phenotype from mouse astrocytes. Biomedicines 2022;10:928

30. Prè D, Nestor MW, Sproul AA, Jacob S, Koppensteiner P, Chinchalongporn V, Zimmer M, Yamamoto A, Noggle SA, Arancio O. A time course analysis of the electrophysiological properties of neurons differentiated from human induced pluripotent stem cells (iPSCs). PLoS One 2014;9:e103418

31. Filippakopoulos P, Knapp S. Targeting bromodomains: epigenetic readers of lysine acetylation. Nat Rev Drug Discov 2014;13:337-356

32. Falkenberg KJ, Johnstone RW. Histone deacetylases and their inhibitors in cancer, neurological diseases and immune disorders. Nat Rev Drug Discov 2014;13:673-691

33. Mazur PK, Herner A, Mello SS, Wirth M, Hausmann S, Sánchez-Rivera FJ, Lofgren SM, Kuschma T, Hahn SA, Vangala D, Trajkovic-Arsic M, Gupta A, Heid I, Noël PB, Braren R, Erkan M, Kleeff J, Sipos B, Sayles LC, Heikenwalder M, Heßmann E, Ellenrieder V, Esposito I, Jacks T, Bradner JE, Khatri P, Sweet-Cordero EA, Attardi LD, Schmid RM, Schneider G, Sage J, Siveke JT. Combined inhibition of BET family proteins and histone deacetylases as a potential epigenetics-based therapy for pancreatic ductal adenocarcinoma. Nat Med 2015;21:1163-1171

34. Korb E, Herre M, Zucker-Scharff I, Darnell RB, Allis CD. BET protein Brd4 activates transcription in neurons and BET inhibitor Jq1 blocks memory in mice. Nat Neurosci 2015;18:1464-1473

35. Dresselhaus EC, Meffert MK. Cellular specificity of NF-κB function in the nervous system. Front Immunol 2019;10:1043

36. Rosenberg SS, Spitzer NC. Calcium signaling in neuronal development. Cold Spring Harb Perspect Biol 2011;3:a004259

37. Macleod GT. Imaging and analysis of nonratiometric calcium indicators at the Drosophila larval neuromuscular junction. Cold Spring Harb Protoc 2012;2012:802-809

38. Berridge MJ. Neuronal calcium signaling. Neuron 1998;21:13-26

39. Greer PL, Greenberg ME. From synapse to nucleus: calcium-dependent gene transcription in the control of synapse development and function. Neuron 2008;59:846-860

40. Fischer I, Dulin JN, Lane MA. Transplanting neural progenitor cells to restore connectivity after spinal cord injury. Nat Rev Neurosci 2020;21:366-383